Molecular Crystals and Liquid Crystals
Publication details, including instructions for authors and subscription information:
http://www.tandfonline.com/loi/gmcl20

Effect of Nanoclay on the Nonisothermal Crystallization of Poly(propylene) and its Blend with Poly[(butylene succinate)-co-adipate]

Jayita Bandyopadhyay [a] & Suprakas Sinha Ray [a b]

[a] DST/CSIR Nanotechnology Innovation Centre, National Centre for Nano-Structured Materials, Council for Scientific and Industrial Research, Pretoria, 0001, South Africa

[b] Department of Chemical Technology, University of Johannesburg, Doornfontein 2018, Johannesburg, South Africa

Available online: 02 Mar 2012

To cite this article: Jayita Bandyopadhyay & Suprakas Sinha Ray (2012): Effect of Nanoclay on the Nonisothermal Crystallization of Poly(propylene) and its Blend with Poly[(butylene succinate)-co-adipate], Molecular Crystals and Liquid Crystals, 556:1, 176-190

To link to this article: http://dx.doi.org/10.1080/15421406.2012.635945

Mol. Cryst. Liq. Cryst., Vol. 556: pp. 176–190, 2012

ISSN: 1542-1406 print/1563-5287 online
DOI: 10.1080/15421406.2012.635945

Taylor & Francis
Taylor & Francis Group

Effect of Nanoclay on the Nonisothermal Crystallization of Poly(propylene) and its Blend with Poly[(butylene succinate)-co-adipate]

JAYITA BANDYOPADHYAY[1] AND SUPRAKAS SINHA RAY[1,2,*]

[1]DST/CSIR Nanotechnology Innovation Centre, National Centre for Nano-Structured Materials, Council for Scientific and Industrial Research, Pretoria 0001, South Africa
[2]Department of Chemical Technology, University of Johannesburg, Doornfontein 2018, Johannesburg, South Africa

The non-isothermal crystallization behaviour and kinetics of neat poly(propylene)(PP), PP/poly[(butylene succinate)-co-adipate] (PP/PBSA) blend and its composite with nanoclay was studied by differential scanning calorimetry at six different cooling rates. Various models, namely the Avrami, the Ozawa and the combined Avrami-Ozawa, were applied to understand the kinetics of the non-isothermal crystallization. All analyses revealed that the rate dependent crystal growth mechanism of neat PP changes after preparation of blend with PBSA and in presence of nanoclay particles in blend composite. Polarized optical microscopy was used to support this conclusion. The activation energy for the non-isothermal crystallization of neat PP, PP/PBSA blend and nanoclay modified PP/PBSA blend composite samples was evaluated by using Kissinger and Augis-Bennett methods. The results showed that the absolute value of the activation energy for the PP matrix crystallization was increased in the case of PP/PBSA blend and this value was dramatically increased in presence of nanoclay. This indicates the slower crystallization kinetics of the PP matrix in presence of nanoclay.

Keywords Nanoclay; nanocomposite; nonisothermal crystallization kinetics; poly(propylene); poly[(butylene succinate)-co-adipate]; polymer blend

Introduction

In the family of commodity plastics, poly(propylene) (PP) is very well-known due to its good cost to properties ratio as well as its versatility. PP is a thermoplastic polyolefin, produced mostly from fossil fuels and ending up as spontaneously undegradable wastes. PP generally degrades in the presence of oxygen and ultraviolet rays [1–3]; however, the degradation process is extremely slow. To date, various approaches have been considered to decrease the use of PP and improve the faster destruction of the product obtained from PP. Among them, the most commonly used method is the blending of PP with a naturally degradable polymer. In this respect, poly[(butylene succinate)-co-adipate] (PBSA) is one

*Address correspondence to Suprakas Sinha Ray, DST/CSIR Nanotechnology Innovation Centre, National Centre for Nano-Structured Materials, Council for Scientific and Industrial Research, Pretoria 0001, South Africa. Tel.: +27 12 841 2388; Fax: +27 12 841 2229. E-mail: rsuprakas@csir.co.za

of the most promising candidates, since it shows a variety of interesting physical properties including biodegradability [1]. However, PP and PBSA are immiscible and their blending leads to materials with weak interfacial adhesion that have poor mechanical performances [1]. The conversion of the PP/PBSA immiscible blend into a useful polymeric product with desirable properties requires some manipulations of the interface.

In recent years, several research groups have reported that organically modified clay can act as a compatibilizer for several types of immiscible polymer blends by effectively reducing the domain size of the minor phase of the blend [1,4–8]. In this direction, we have melt-blended PP with PBSA in absence and presence of organoclay, and have studied the morphology, structure, and properties thereof [1]. Results showed that the incorporation of 5 wt.% organoclay into the PP/PBSA blend changes the blend morphology from highly phase-separated to a typical co-continuous structure. Such observation was attributed to the selective localization of intercalated silicate layers in the PBSA phase, which finally increases the viscosity ratio of the blend matrices [1]. As a result, the organoclay-modified PP/PBSA blend showed a much bigger improvement in mechanical, thermal and rheological properties than that of unmodified PP/PBSA blend or neat PP.

A pertinent question is how does this morphological change affect the crystal growth of PP matrix during non-isothermal cryatallization? The understanding of polymer crystallization behaviour under dynamic conditions is of great importance, because most industrial processing techniques actually occur under non-isothermal conditions. Moreover, non-isothermal crystallization can broaden and supplement the knowledge of the crystallization behaviour of polymeric materials.

Therefore, the main objective of this study is to understand the effect of clay particles on the non-isothermal crystallization behaviour and kinetics of neat PP upon blend composite formation with PBSA and organoclay. Different theoretical approaches have been used to describe the kinetics of non-isothermal crystallization.

Experimental

Materials

The PBSA used in this study was a commercial product from Showa High Polymer Ltd., Japan, with the designation BIONOLLE #3001 ($M_w = 190$ kg/mol). The PP matrix used was a homopolymer Pro-fax PDC 1274 (DuPont Canada, $M_w = 250$ kg /mol).

The organically modified clay used in this study was Cloisite®20A (commercially abbreviated as C20A), supplied by the Southern Clay Products. According to the supplier the original clay was Na^+–MMT and intercalated with 38 wt.% of N,N-dimethyldihydrogenated tallow ammonium chloride salt. Tallow is a mixture of octadecyl, hexadecyl, and tetradecyl with octadecyl being the major component (>60%) [9].

Sample Preparation

Blend (PPB) and C20A-containing blend composite (PPBNC) were prepared by first melting the polymers and then mixing of C20A for 10 min in a Thermohaake twin-rotors mixer (Polylab system) at 190°C and a rotor speed of 60 rpm. The blends were then compression moulded using a Carver laboratory press at 190°C for 10 min into 1.5 mm thick sheets and then cooled to room temperature. The weight ratio of PP and PBSA in PPB was 80/20. In PPBNC, the weight ratio of PP: PBSA: C20A was 80:20:5.

Characterization Techniques

The crystallization behaviours and kinetics of PP, PPB and PPBNC were studied by means of differential scanning calorimeter (DSC, model Q2000 TA Instruments) under constant nitrogen flow of 50 ml/min. The sample weight was maintained at low levels (3.6–4.1 mg) for all measurements in order to minimize any possible thermal lag during the scans. In addition, all samples were weighed in such a way that the amount of polymer matrix was the same. The temperature and heat of fusion of DSC were calibrated with an indium standard, and the base line was checked according to TA Instruments protocols. The samples were heated from 0°C to 185°C at a heating rate of 20°C/min and kept at this temperature for 3 min. After that, the samples were cooled to 0°C at different cooling rates ($\phi = 1$, 2, 5, 10, 15 and 20°C/min) and then heated immediately to 185°C at a heating rate of 20°C/min as soon as each sample had finished cooling. The data reported here are representative of three independent tests.

In order to support the nonisothermal crystallization studied by DSC, the polarized optical microscopy (POM) was employed. In this experiment, the samples, which were sandwiched between two glass cover-slips, were placed in a Linkam temperature controlled device and then heated from room temperature to 185°C at a heating rate of 20°C/min. The samples were kept at this temperature for 3 min. Afterwards, the samples were cooled to room temperature at a cooling rate of 10°C/min. Reported POM images of various samples were taken at 120°C during cooling from their melts. To check their reproducibility, for each sample, this experiment was also repeated independently three times.

Results and Discussion

Non-Isothermal Crystallization Behaviour

The study of non-isothermal crystallization kinetics of polymeric materials is essential since most of the industrial processing techniques follow this behaviour. The detailed experimental procedure is described in the characterization part and the non-isothermal crystallization behaviour of neat PP, PPB, and PPBNC are illustrated in Fig. 1. Furthermore, the results are summarised in Table 1. According to the Table 1, the onsets of crystallization temperature ($T_{c,on}$) for all samples studied here, are shifting towards the lower temperature region with an increase in the cooling rate. Such an observation is very usual, since at a slower rate, the molten samples get more time to start the crystallization process at higher temperature compared to the faster rate. At slow cooling rates ($\phi = 1$, 2 and 5°C/min), the crystal growth starts (refer to $T_{c,on}$ of Table 1) almost at the same temperature in the case of PP and PPBNC. But in the case of PPB, the crystallization starts at a higher temperature compared to the neat PP or PPBNC. At faster rates, $T_{c,on}$ of PPB and PPBNC become comparable and it is greater than neat PP. Therefore, the nucleation efficiency is highest in PPB. It decreases in the presence of clay (i.e., in case PPBNC) at slower rates and then becomes comparable with PPB at higher cooling rates.

The crystallization peak temperature ($T_{c,1}$) also moves toward the lower temperature with an increase in the cooling rate. This is quite obvious because the systems don't get enough time to start the crystallization process at a higher temperature during fast cooling. Although the crystal growth initially starts almost at the same temperature ($T_{c,on}$), in the case of both neat PP and PPBNC (especially at slower rates), $T_{c,1}$ for PPBNC always remains higher than that of neat PP. Again, a cooling rate of 1°C/min, $T_{c,1}$ follows the trend PPB >

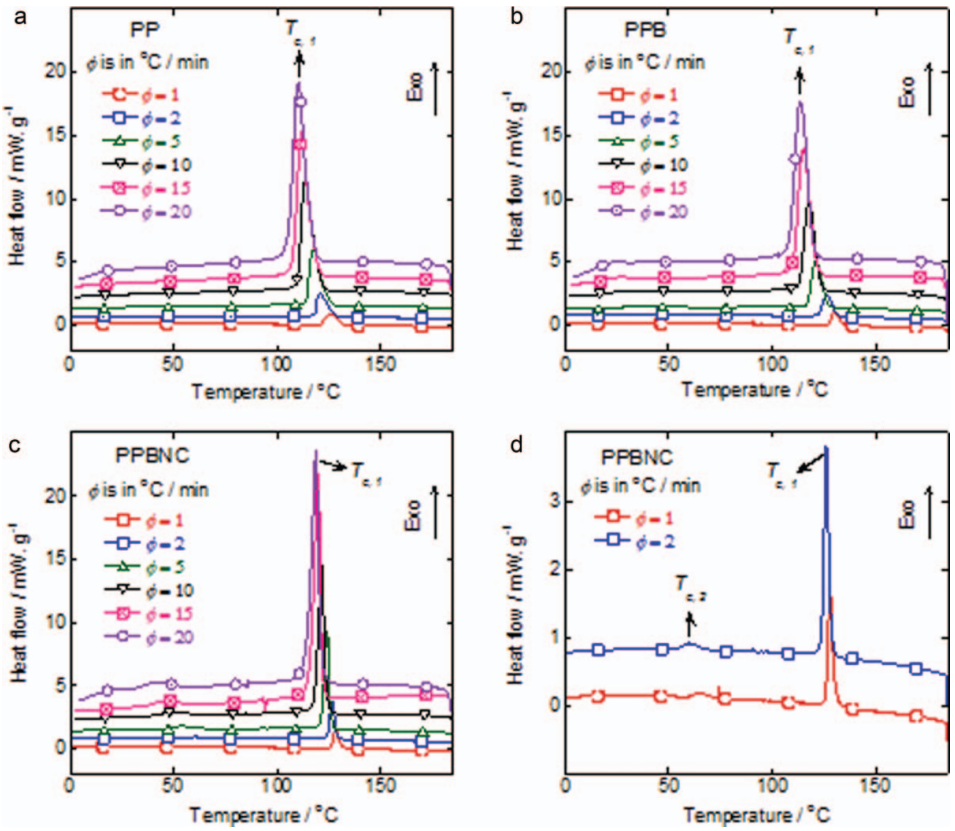

Figure 1. Differential scanning calorimetric exotherms of: (a) neat PP, (b) PPB and (c) PPBNC during nonisothermal crystallization at different cooling rates. (d) Exotherms of PPBNC at slower cooling rates show the presence of another exothermic peak at lower temperature along with the sharp crystal peaks at higher temperature.

PPBNC > PP. This trend changes to PPB ≈ PPBNC > PP at a cooling rate of 2°C/min. Afterwards, the trend remains the same for all cooling rates examined as PPBNC > PPB > PP. This indicates that PBSA in PPB and PPBNC mainly acts as a nucleating agent to start crystallization. But the nucleation efficiency of intercalated silicate layers, in the case of PPBNC, plays an important role during faster cooling.

Although both clay and PBSA act as nucleating agents, the overall growth of crystals decreases in PPB and PPBNC as compared to neat PP. As a result, $\Delta H_{c,1}$ of neat PP decreases after a preparation of blend and blend composite with C20A. In PPBNC, the clay-polymer interaction is more favourable in the case of PBSA than in PP [1]. Furthermore, according to the scanning electron microscopic (SEM) images, the immiscible structure of a blend significantly changes to a typical oriented co-continuous morphology (refer to Fig. 2). This could be the result of either the common intercalation of both polymer chains in the clay galleries, an insertion of one component of blend in the clay galleries, or the change in the viscosity ratio of blend components depending on the intercalation of blend components in the clay galleries [1]. Again, it is well known that the incorporation of any foreign material

Table 1. Characteristic parameters of Nonisothermal Crystallization of neat PP, PPB and PPBNC

Sample	ϕ/°C. min^{-1}	$T_{c,\,on}$ /°C	$T_{c,\,1}$ /°C	$\Delta H_{c,\,1}$ /J.g^{-1}	$T_{c,\,2}$ /°C	$\Delta H_{c,\,2}$ /J.g^{-1}	T_{m1} /°C	T_{m2} /°C	T_{m3} /°C	ΔH_f /J.g^{-1}
PP	1	137.10	125.61	91.38					163.30	96.96
	2	135.49	120.40	91.26					161.83	97.19
	5	130.42	117.31	94.56					160.79	96.36
	10	128.75	113.29	94.51					160.11	94.65
	15	126.60	111.52	89.78					159.95	89.93
	20	125.17	110.08	89.90					159.86	87.69
PPB	1	142.59	129.99	78.81				92.24	164.38	96.61
	2	140.68	126.21	75.20				92.53	163.65	91.80
	5	138.53	121.33	74.48				92.82	161.97	88.04
	10	134.71	117.66	77.30				92.24	161.03	88.99
	15	130.89	115.20	79.48				92.72	160.29	89.57
	20	128.98	113.75	79.04				92.79	159.69	89.84
PPBNC	1	136.62	127.95	71.58			84.42	94.30	163.63	87.00
	2	134.23	126.19	65.86	60.36	6.15	82.10	94.88	163.68	79.55
	5	131.85	123.84	70.73	53.73	6.76		93.43	162.34	82.08
	10	131.13	121.32	70.02	48.63	5.83		92.72	161.09	81.44
	15	130.42	119.42	75.57	44.65	4.44		92.48	161.01	88.43
	20	130.18	118.43	71.32	40.53	4.22		92.56	161.03	82.39

$T_{c,\,on}$, crystallization onset temperature; $T_{c,\,1}$, first crystallization peak temperature; $\Delta H_{c,\,1}$, enthalpy of crystallization of first crystal peak; $T_{c,\,2}$, second crystallization peak temperature; $\Delta H_{c,\,2}$, enthalpy of crystallization of second crystal peak; T_{m1}, first melting peak; T_{m2}, second melting peak; T_{m3}, third melting peak; ΔH_f, enthalpy of fusion.

in the matrix polymer may act as a nucleating agent [10]. For these reasons, in the case of PPB, the PBSA acts as a nucleating agent. However, due to the immiscible structure of blend, the overall growth of crystals gets hindered. Hence $\Delta H_{c,1}$ of PPB decreases in comparison to neat PP and then the incorporation of clay in the blend matrix further hinders

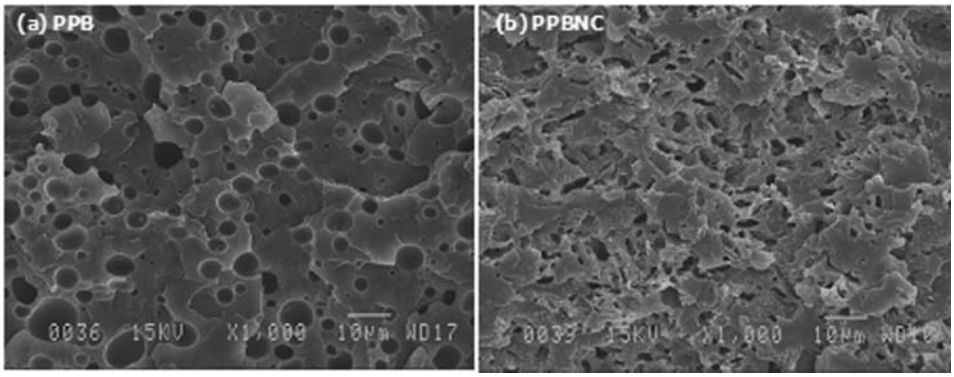

Figure 2. Fracture surface image of (a) PPB and (b) PPBNC.

the crystal growth mechanism. For this reason, the $\Delta H_{c,1}$ value further decreases in the case of PPBNC.

According to Fig. 1 and Table 1, a single crystal peak appeared for neat PP and PPB during the cooling cycle from their melts. In the case of PPBNC, another very small crystal peak appeared at a much lower temperature range along with the main crystal peak (refer to Fig. 1(d)). Such a small peak is related to the crystallization of PBSA phase (crystallization temperature of neat PBSA = 56.8°C [11]) in the presence of clay particles as PBSA has a more favourable interaction with C20A surface than the PP phase. The peak temperature and enthalpy of PBSA crystallization are tabulated in Table 1 as $T_{c,2}$ and $\Delta H_{c,2}$, respectively. With an increase in the cooling rate, this $T_{c,2}$ shifts towards the lower temperature. Besides this, $\Delta H_{c,2}$ reduces with an increase in the cooling rate.

The melting peak temperatures and the enthalpy of fusion during successive heating scans are also tabulated in Table 1. According to the calculated data, a single melting peak appeared for neat PP ($T_{m,3}$), a double melting behaviour ($T_{m,3}$ and $T_{m,2}$) can be observed for PPB and PPBNC with higher cooling rates. In the case of PPBNC, at slower rates ($\phi = 1$ and 2°C/min) a triple melting ($T_{m,3}$, $T_{m,2}$ and $T_{m,1}$) behaviour can be observed. $T_{m,3}$, $T_{m,2}$ and $T_{m,1}$ are representing melting peaks from higher to lower temperatures. PBSA usually shows double melting behaviour with a main melting peak at 94.5°C and a shoulder at 83.1°C. Therefore, in the case of PPB and PPBNC, $T_{m,2}$ and $T_{m,1}$ appeared due to the melting of PBSA crystals. The growth of this PBSA crystal in the case of PPBNC is clearly visible in the cooling exotherms of Fig. 1. Since $T_{m,2}$ is very close to the melting peak of PBSA, both PP and PBSA crystals may be growing at the same time under a single exothermic peak during cooling. In case of PPBNC, the same phenomenon is happening for all the cooling rates studied here. But in case of PPBNC, another interesting phenomenon is also happening at the slower cooling rates. The effect of intercalation of PBSA chains alone in the clay galleries can be observed from the appearance of a separate exothermic peak near the crystallization temperature of PBSA. Further, $T_{m,3}$ of neat PP shifted toward the higher temperature after the preparation of blend and blend composite with C20A. The total enthalpy of fusion (ΔH_f) (estimated by considering all the melting) is showing the similar trend like $\Delta H_{c,1}$. On the basis of these results, the morphology of the blend and blend composite can be modelled according to Fig. 3. As depicted in Fig. 3, in PPBNC, the PBSA chains mainly get intercalated into the clay galleries and create co-continuous morphology (refer Fig. 2) of PPBNC [1].

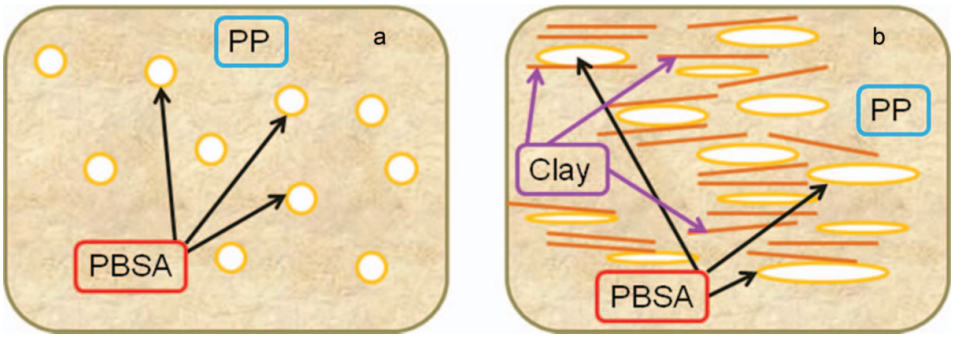

Figure 3. Morphological model of (a) PPB and (b) PPBNC. PP is the matrix polymer and PBSA is the minor component of a blend. In the presence of clay in PPBNC, the PBSA phase is deformed and some of the PBSA chains become intercalated in the clay galleries.

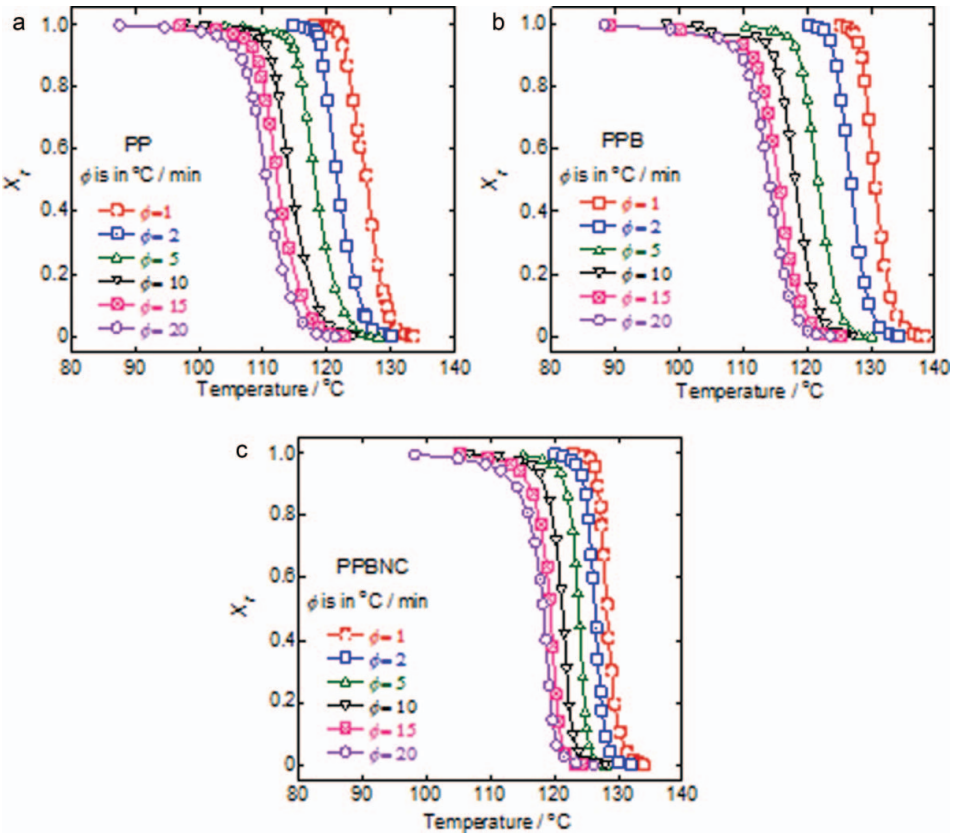

Figure 4. The relative degree of crystallinity (X_T) versus temperature plots for (a) PP, (b) PPB, and (c) PPBNC at various cooling rates during the nonisothermal crystallization.

Non-Isothermal Crystallization Kinetics

The first step in studying the non-isothermal crystallization is to determine the relative degree of crystallinity as a function of temperature (X_T) and time (X_t) as presented in Figs. 4 and 5, respectively. X_T can be defined as:

$$X_T = \frac{\int_{T_o}^{T} (dH_c/dT)dT}{\int_{T_o}^{T_\alpha} (dH/dT)dT} \tag{1}$$

where T_o ($T_{c,\,on}$) and T_α ($T_{c,\,fin}$) are the initial and final temperature of crystallization. To see the change of relative degree of crystallinity as a function of time (X_t), the temperature scale was transformed into time scale by using equation 2.

$$t = (T_o - T)/\phi \tag{2}$$

where T_o represents the onset temperature of crystallization and T is the same temperature used to determine X_T. As a function of time or temperature, the value of relative degree of crystallinity remained the same, the suffix only denotes the abscissa. Crystallization

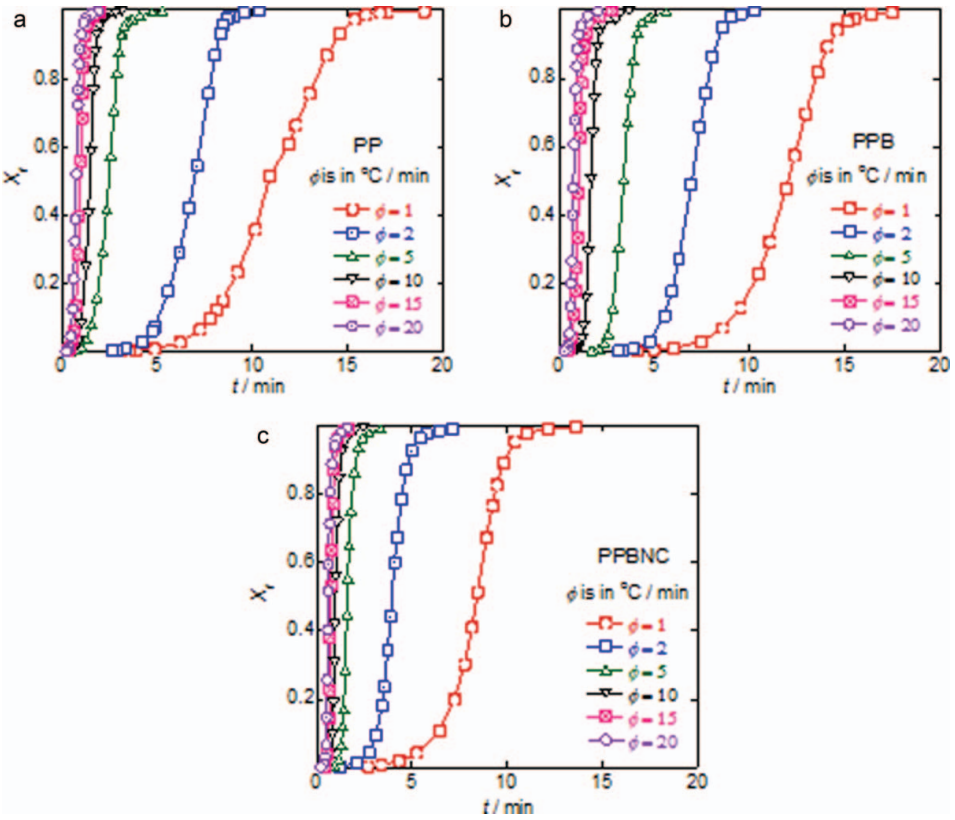

Figure 5. The relative degree of crystallinity (X_t) versus time plots for: (a) PP, (b) PPB, and (c) PPBNC at various cooling rates during the nonisothermal crystallization.

kinetics was then analyzed by using different models such as the Ozawa, the Avrami, and the Liu.

Nonisothermal Crystallization Kinetics by Ozawa Model

Truncating the non-isothermal crystallization process into infinitesimally small isothermal process, Ozawa extended the Avrami model for isothermal crystallization to analyse non-isothermal crystallization kinetics [12]. According to this model, X_T can be written as a function of cooling rate as:

$$\ln[-\ln(1 - X_T)] = \ln K(T) - m \ln \phi \tag{3}$$

where *K(T)* represents Ozawa crystallization rate constant and m is the Ozawa exponent depending on the dimension of crystal growth. Therefore, the plot $\ln[-\ln(1 - X_T)]$ versus $\ln \phi$ should be a straight line if this model is valid. *K(T)* and m can be estimated from the anti-logarithmic value of the y-intercept and slope, respectively. According to the Ozawa plot (refer to Fig. 6), the Ozawa model fails to describe the non-isothermal crystallization kinetics for the present systems at higher temperatures. But at the end of the crystallization

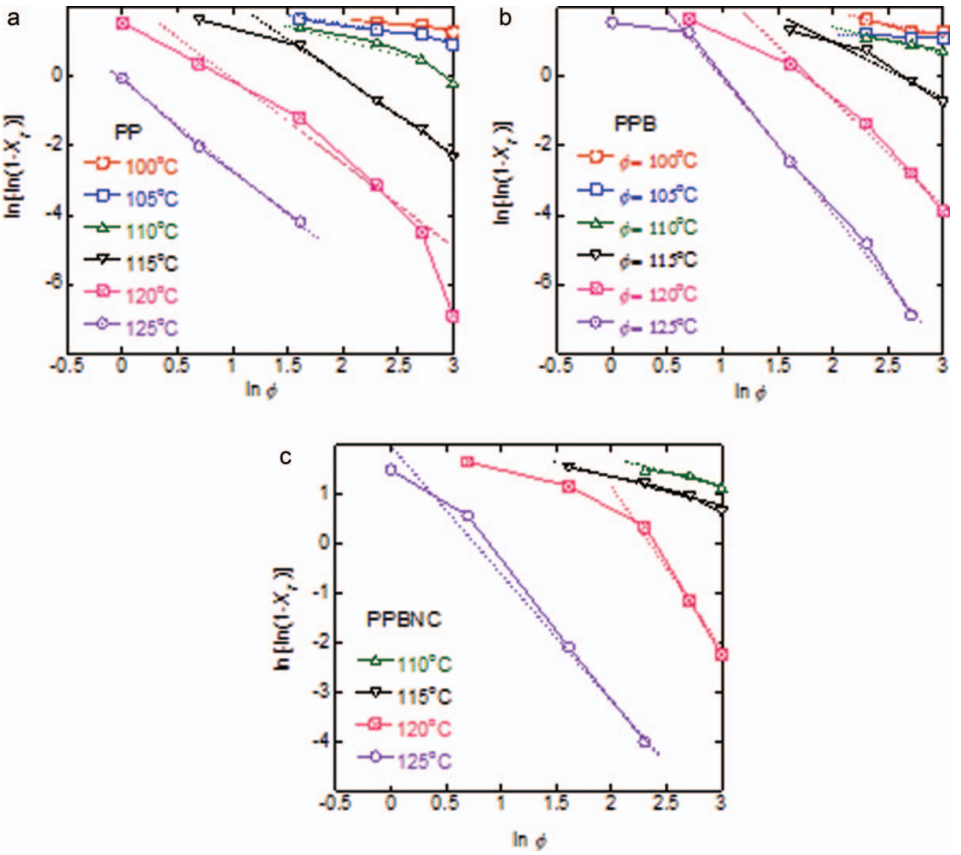

Figure 6. $\ln[-\ln(1 - X_T)]$ versus $\ln \phi$ plots for: (a) PP, (b) PPB and (c) PPBNC.

process (at lower temperatures), this model works nicely. It should be kept in mind that in this model, the effect of secondary crystallization was not taken into account [13]. Due to this, the Ozawa analysis (developed to analyze nonisothermal crystallization kinetics) is not valid during crystal growth at higher temperatures. Therefore, as an alternative method, the Avrami model was used to understand the non-isothermal crystallization kinetics of blend systems [14].

Nonisothermal Crystallization Kinetics by the Avrami Model

According to the Avrami model the equivalent time dependent crystallinity can be expressed as,

$$\ln [-\ln (1 - X_t)] = \ln\ Z_t + n\ \ln\ t \tag{4}$$

where Z_t is a composite rate constant involving both nucleation and growth rate parameters and the Avrami exponent n is a constant depending on the type of nucleation and growth process [15]. Equation 4 represents a straight line and Z_t and n can be determined from the antilogarithmic value of the y-intercept and slope, respectively. Please note that here Z_t and n don't possess the same physical meaning as the original Avrami analysis for

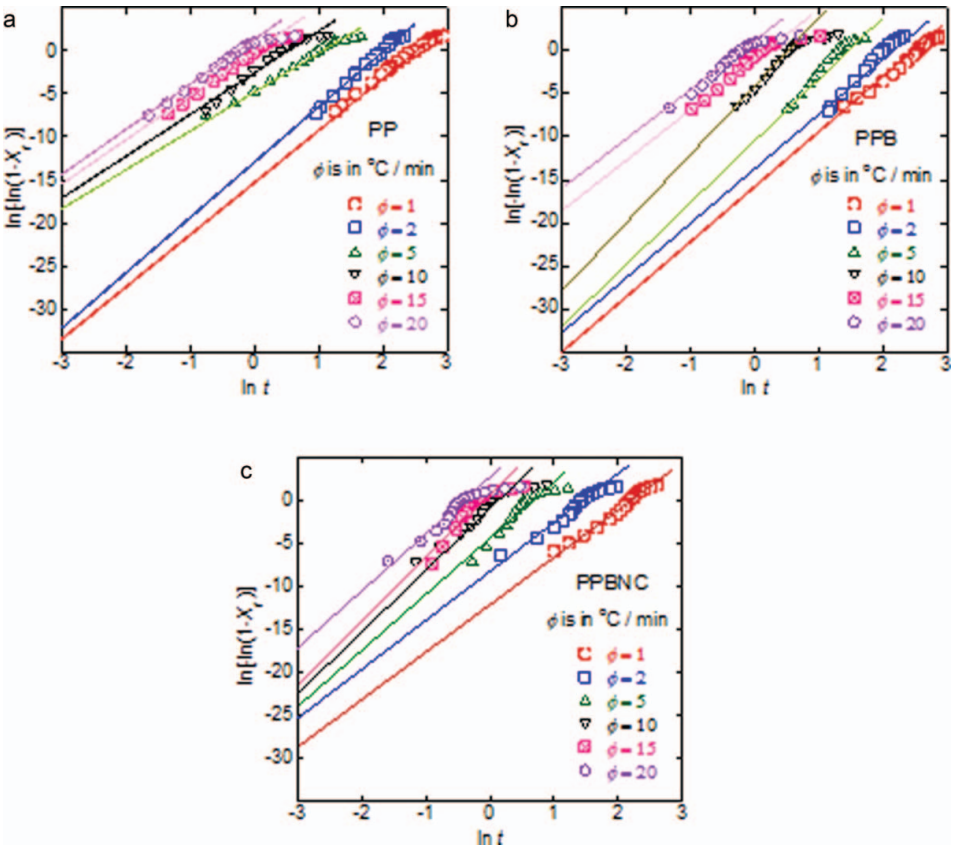

Figure 7. $\ln[-\ln(1 - X_t)]$ versus $\ln t$ plots for: (a) PP, (b) PPB, and (c) PPBNC.

isothermal crystallization because the temperature changes instantly in a nonisothermal process. Here, they are adjustable parameters to fit the experimental results and help to analyze crystallization kinetics.

In parts (a), (b), and (c) of Fig. 7, $\ln[-\ln(1 - X_t)]$ was plotted against $\ln t$ to check the validity of Avrami model for the neat PP, PPB and PPBNC, respectively. According to this figure, the Avrami model can describe the crystallization kinetics of neat PP, PPB, and PPBNC successfully over the straight line range. The deviation from a straight line in the longer time scale is due the impingement of the crystals–commonly known as secondary crystallization. From this figure, it is clear that for all the samples, the secondary crystallization becomes more prominent with an increase in the cooling rate.

The parameters n and $\ln Z_t$ are tabulated in Table 2. Jeziorny suggested that the parameter Z_t should be modified when Avrami analysis is applied to explain the nonisothermal crystallization kinetics. Assuming a constant or almost constant cooling rate, the final form of this parameter suggested by Jeziorny is [16]:

$$\ln Z_c = (\ln Z_t)/\phi \tag{5}$$

According to Table 2, the n-values for all the samples are cooling rate dependent. At $\phi = 1^{\circ}$C/min, n-values follows the trend PPB > PP > PPBNC. Again, this suggests the

Table 2. Kinetic parameters based on Avrami and Zeziorny analyses

Sample	Rate	n	ln Z_t	ln Z_c
PP	1	6.15	−33.63	−33.63
	2	5.10	−32.14	−16.07
	5	4.60	−18.23	−3.65
	10	4.84	−17.11	−1.71
	15	3.48	−15.25	−1.02
	20	3.48	−14.25	−0.71
PPB	1	6.52	−34.86	−34.86
	2	6.34	−32.89	−16.45
	5	7.08	−31.89	−6.38
	10	5.67	−27.92	−2.79
	15	5.84	−18.48	−1.23
	20	5.65	−15.87	−0.79
PPBNC	1	5.51	−28.54	−28.54
	2	5.72	−25.31	−12.66
	5	6.58	−23.82	−4.76
	10	7.15	−22.45	−2.25
	15	7.39	−21.34	−1.42
	20	6.66	−16.99	−0.85

Z_t, is a composite rate constant involving both nucleation and growth rate parameters; n, Avrami exponent is a constant depends on the type of nucleation and growth process; ln Z_c = (ln Z_t)/ϕ.

nucleation efficiency is highest in the case of PPB at this cooling rate. At $\phi = 2^\circ$C/min and 5°C/min this trend changes to PPB > PPBNC > PP. A further increase in the cooling rate results in slightly higher n-values for PPBNC compared to PPB. But at higher cooling rates, n-values of PPB and PPBNC are much higher than neat PP. This trend is very similar to the $T_{c,on}$.

Although ln Z_t and hence ln Z_c are adjustable parameters, they provide some information on the growth rate of spherulites. According to Table 2, it changes with the cooling rate. For $\phi = 1^\circ$C and 2°C/min, ln Z_c follows the trend PP ≈ PPB > PPBNC. At 5°C/min PPB > PPBNC > PP. For other rates, the growth rate of spherulites becomes almost constant in all of the samples.

Nonisothermal Crystallization Kinetics by Liu Model

By combining all the variables employed to describe the nonisothermal crystallization process, Liu et al. proposed a model represented by the equation 6 [17]:

$$\ln Z_t + n \ln t = \ln K(T) - m \ln \phi \tag{6}$$

By rearranging equation 6, the final form becomes

$$\ln \phi = \ln F(T) - a \ln t \tag{7}$$

where, $F(T) = [K(T)/Z_t]^{1/m}$ refers to a cooling rate to reach a defined degree of crystallinity and a is the ratio of the Avrami exponent to the Ozawa exponent, *i.e.* $a = n/m$. For a given

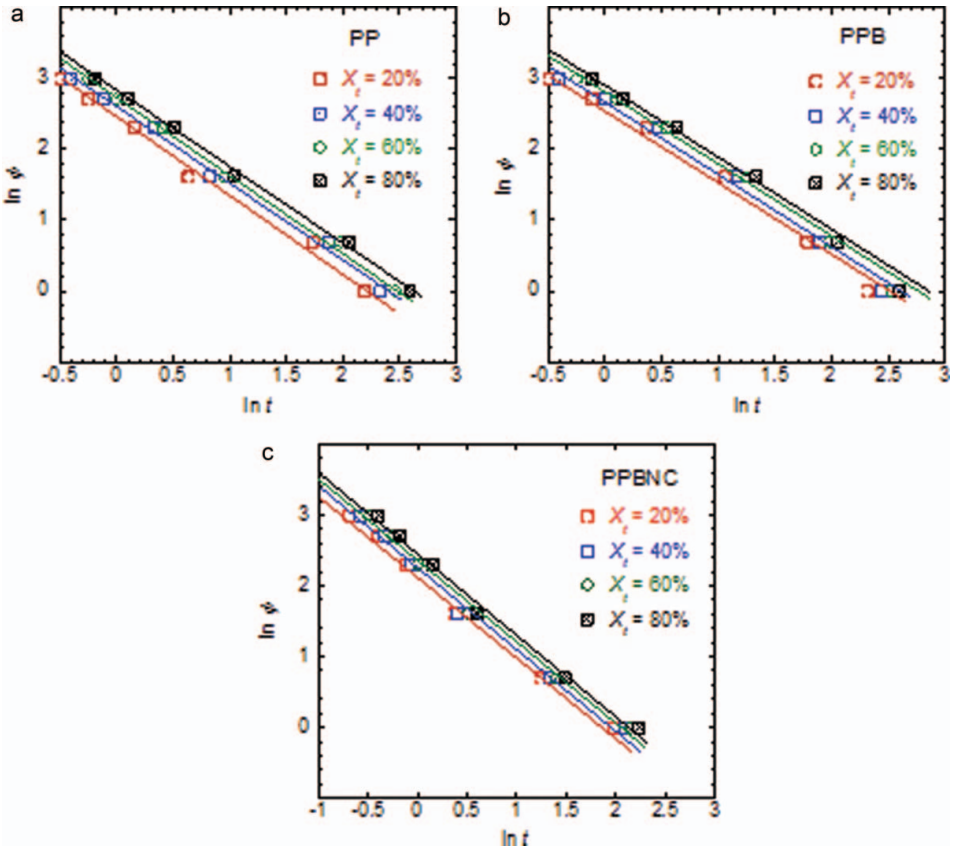

Figure 8. ln ϕ versus ln t plots for: (a) PP, (b) PPB and (c) PPBNC.

degree of crystallinity, $F(T)$ and a can be determined from the y-intercept and slope of the straight lines defined by equation 7. Figure 8 shows the Liu analysis is valid for neat PP, PPB, and PPBNC. According to Table 3, the values of the kinetic parameters $F(T)$ and a increased a little in PPBNC for all the values of the relative degree of crystallinity

Table 3. Kinetic parameters based on Liu model

		Degree of crystallinity			
Sample	Kinetic parameter	20%	40%	60%	80%
PP	*F(T)*	3.01	3.13	3.27	3.38
	a	1.11	1.08	1.10	1.10
PPB	*F(T)*	3.05	3.16	3.30	3.39
	a	1.03	1.02	1.02	1.01
PPBNC	*F(T)*	3.24	3.39	3.49	3.60
	a	1.14	1.16	1.15	1.15

$F(T) = [K(T)/Z_t]^{l/m}$ refers to a cooling rate to reach a defined degree of crystallinity and a is the ratio of Avrami exponent to Ozawa exponent, *i.e.* $a = n/m$.

compared to PP and PPB. This indicates a comparison to neat PP or PPB; in PPBNC at unit crystallization time a higher cooling rate is necessary to obtain a certain degree of crystallinity.

Determination of Activation Energy for the Nonisothermal Crystallization

The activation energy (ΔE) for nonisothermal crystal growth was determined on the basis of the Kissinger and Augis–Bennett methods and both are represented by the following equations:

Kissinger method [18]:

$$\frac{d\left[\ln\left(\phi/T_c^2\right)\right]}{d(1/T_c)} = -\frac{\Delta E}{R} \tag{8}$$

Augis–Bennett method [19]:

$$\frac{d[\ln(\phi/(T_o - T_c))]}{d(1/T_c)} = -\frac{\Delta E}{R} \tag{9}$$

Considering the variation of T_c (in Kelvin) with ϕ, the activation energy (absolute value of ΔE) was estimated from the slopes (represented by equations 8 and 9) of the least square lines. In this calculation, T_{c1} was considered as T_c and $T_{c,\,\mathrm{on}}$ as T_0. Figure 9 illustrates the least square plots representing the Kissinger and Augis–Bennett methods. Corresponding ΔE values were reported in Table 4. The value of universal gas constant used for the calculation is 0.0083 KJ/(g.mol.K). According to Table 4, the activation energy necessary to start the crystal growth process remains almost the same in PP and PPB. But it increases a lot in the case of PPBNC. This indicates that organoclay decelerates the crystal growth of the PP matrix in PPBNC. Again, this supports the fact that nucleation efficiency and the overall crystal growth of PP matrix is reduced in PPBNC.

According to Table 4, for every sample there is a discrepancy in the activation energy determined by the Kissinger and Augis-Bennett method. In the Augis-Bennett method, there are two assumptions: first, $\Delta E >> RT$ (i.e., $\Delta E/RT \approx \infty$); and second, $(T_{1/2})_1 (T_{1/2})_2 \approx {T_c}^2$ [20]. Where $(T_{1/2})_1$ and $(T_{1/2})_2$ are the temperatures at the half maximum

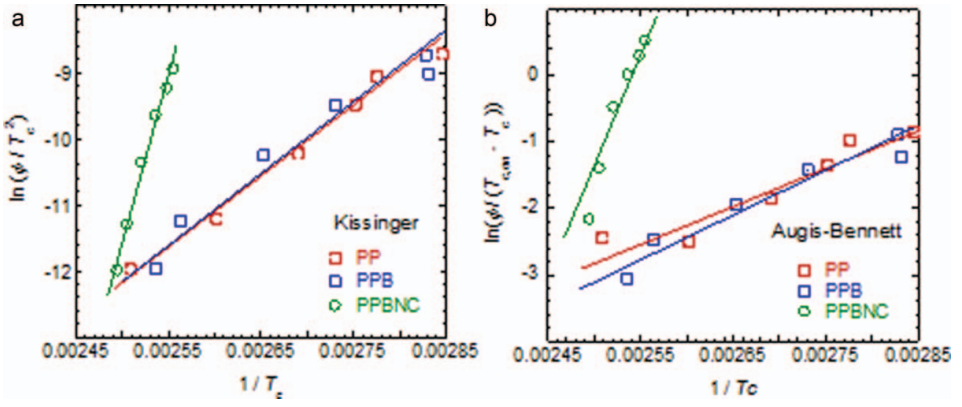

Figure 9. Determination of activation energies describing the nonisothermal crystallization process for PP, PPB and PPBNC based on: (a) Kissinger, (b) Augis-Bennett methods.

Table 4. Activation energy for the overall nonisothermal crystallization of PP, PPB and PPBNC

	Activation energy, $-\Delta E$/KJ.mol^{-1}	
Sample	Kissinger	Augis-Bennett
PP	89.23	47.73
PPB	90.06	56.03
PPBNC	423.30	280.87

before and after the crystallization peak. The determination of the activation energy by the Augis-Bennett method is really fruitful, providing the reaction obeys the Avrami law. On the other hand, the Kissinger model is assumption free. Therefore, for the present study the Kissinger approach is the most reliable.

Spherulitic Growth Behaviour

In order to support the crystal growth behaviour analyzed by DSC, POM observations were carried out under nonisthermal conditions. Figure 10 shows the POM images of all the

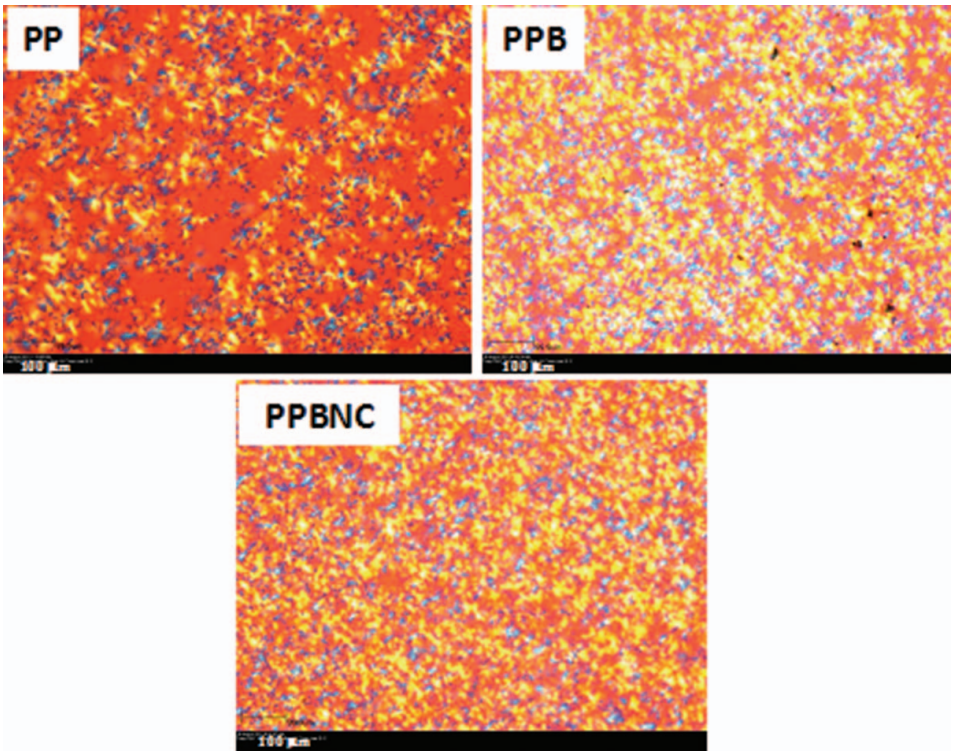

Figure 10. Polarized optical microscopic images of PP, PPB and PPBNC crystals grew at 120°C during cooling.

samples taken at 120°C during nonisothermal crystallization at a rate of 10°C/min from their melts. According to POM images, the growth of spherulites in neat PP was fairly large and they were more perfectly grown. In the case of PPB, small crystals grew due to a higher nucleation efficiency. On the other hand, in the case of PPBNC, some larger spherulites of PP grew along with the smaller crystallites. Again, these observations supported that idea that the nucleating efficiency increases in PPB in the presence of PBSA, but it reduces in the presence of clay in the PPBNC.

Conclusion

The effect of the degree of intercalation of polymer chains in the clay galleries on the nonisothermal crystallization of blend/clay nanocomposite is reported in this article. The detailed nonisothermal crystallization behaviour and kinetics of neat PP, PPB and PPBNC were studied using DSC and POM. Results show that although PBSA acts as a nucleating agent, the overall crystal growth decreases in PPB. Again, in PPBNC, due to some intercalation of PBSA chains in the clay galleries, the overall crystal growth is hindered. For this reason, some PP crystals can grow separately at the beginning of the crystallization process of PPBNC as revealed by POM images. Therefore, in conclusion, although the morphology of PPB changes to a co-continuous structure after incorporation of clay in PPBNC, the compatibilization/common intercalation of both polymers in the clay galleries didn't occur properly. Hence, in PPB, during cooling from the melt, both PP and PBSA crystals grow under a single exotherm. PPBNC shows similar behaviour like PPB for all the cooling rates studied here, but at slower cooling rates the effect of intercalation of PBSA chains alone in the clay galleries can be observed from the appearance of a separate exothermic peak near the crystallization temperature of PBSA.

References

[1] Sinha Ray, S., Bandyopadhyay, J., & Bousmina, M. (2007). *Macromol. Mater. Eng.*, *292*, 729.
[2] Guillet, J. (1984). *Encyclopedia of Chemical Technology*, Wiley-Interscience: New York, p. 626.
[3] Albertsson, A. C., Barenstedt, C., Karlsson, S., & Lindberg, T. (1995). *Polymer.*, *36*, 3075.
[4] Sinha Ray, S., Bousmina, M., & Maazouz, A. (2006). *Polym. Eng. Sci.*, *46*, 1121.
[5] Sinha Ray, S., & Bousmina, M. (2005). *Macromol. Rapid Commun.*, *26*, 450.
[6] Sinha Ray, S., & Bousmina, M. (2005). *Macromol. Rapid Commun.*, *26*, 1639.
[7] Sinha Ray, S., Pouliot, S., Bousmina, M., & Utracki, L. A. (2004). *Polymer*, *45*, 8403.
[8] Si, M., Araki, T., Ade, H., Kilcoyne, A. L. D., Fisher, R., Sokolov, J. C., & Rafailovich, M. H. 312 (2006). *Macromolecules*, *39*, 4793.
[9] Data sheet, Southern Clay Product Inc.: Texas.
[10] Ojijo, V., Cele, H., & Sinha Ray, S. (2011). *Macromol. Mater. Engg.*, *196*, in press.
[11] Bandyopadhyay, J., Sinha Ray, S., & Bousmina, M. (2007). *J. Nanosci. Nanotechnol.*, *8*, 1812.
[12] Ozawa, T. (1971). *Polymer*, *12*, 150.
[13] Zhizhong, S., Weihong, G., Yongjun, L., Qiuying, L., & Chifei, W. (2009). *Polym. Bull.*, *62*, 629.
[14] Chen, G.-X., & Yoon, J.-S. (2005). *J. Polym. Sci., Part B: Polym. Phys.*, *43*, 817.
[15] Avrami, M. J. (1940). *Chem. Phys.*, *8*, 212.
[16] Jeziorny, A. (1978). *Polymer*, *19*, 1142.
[17] Liu, T. X., Mo, Z. S., Wang, S. E., & Zhang, H. F. (1997). *Polym. Eng. Sci.*, *37*, 443.
[18] Kissinger, H. E. (1965). *J. Res. Natl. Bur. Stand.*, *57*, 217.
[19] Augis, J. A., & Bennett, J. E. (1978). *J. Therm. Anal.*, *13*, 283.
[20] Gotor, F. J., & Criado, J. M. (2001). *J. Am. Ceram. Soc.*, *84*, 1797.